Rhizophora-based Particleboard Bonded with Soy Flour and Lignin as Potential Phantom
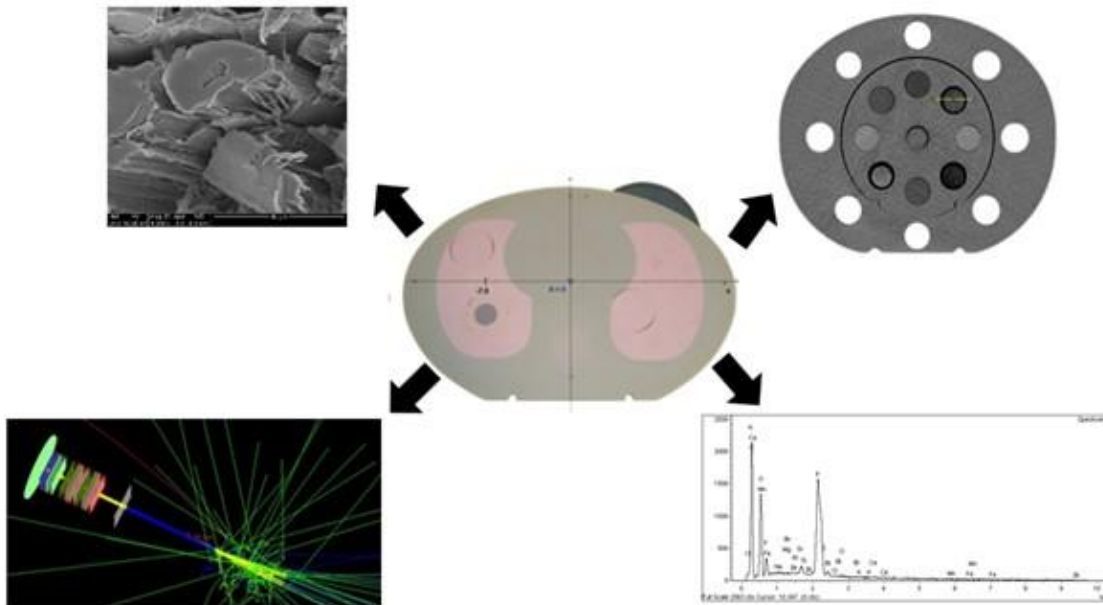
Siti Hajar Zuber,[a,*] Muhammad Fahmi Rizal Abdul Hadi,[b] Nurul Ab. Aziz Hashikin,[b] Mohd Fahmi Mohd Yusof,[c] and Mohd Zahri Abdul Aziz [d]

Corresponding author: hajarzuber@ukm.edu.my

GRAPHICAL ABSTRACT

Rhizophora-based Particleboard Bonded with Soy Flour and Lignin as Potential Phantom

Siti Hajar Zuber,[a,*] Muhammad Fahmi Rizal Abdul Hadi,[b] Nurul Ab. Aziz Hashikin,[b] Mohd Fahmi Mohd Yusof,[c] and Mohd Zahri Abdul Aziz [d]

Rhizophora-based particleboard was evaluated for its suitability as phantom material, especially in medical physics applications. The elemental composition, effective atomic number, micrographic structures, computed tomography (CT), and attenuation properties of *Rhizophora*-based particleboards were examined. These investigations considered three different particle sizes and three distinct adhesive mixtures. *Rhizophora* sample at particle sizes of 0 to 103 μm, with 4.5% soy flour and 1.5% lignin (C_6) presented with a homogenous compound with better uniformity compared with other samples, and *Rhizophora* sample at particle sizes of 104 to 210 μm, with 9% soy flour and 3% lignin (B_{12}) demonstrated an effective atomic number of 8.15, which is similar to water. C_6 also presented with a density distribution profile with close proximity to water. The measured attenuation coefficients of samples were aligned closely with those of water, as determined by XCOM. The results suggest that the formulation of soy flour and lignin as adhesives for *Rhizophora*-based particleboard is suitable for the fabricating of phantom material for medical physics applications, especially mainly due to its natural origin.

*Contact information: a: Centre for Diagnostic, Therapeutic and Investigative Studies, Faculty of Health Sciences, Universiti Kebangsaan Malaysia, 50300, Kuala Lumpur, Malaysia; b: School of Physics, Universiti Sains Malaysia, 11800, Penang, Malaysia; c: Faculty of Health and Life Sciences, Management & Science University, 40150 Shah Alam, Selangor, Malaysia; d: Pusat Perubatan USM, Universiti Sains Malaysia, 13200, Penang, Malaysia; *Corresponding author: hajarzuber@ukm.edu.my*

INTRODUCTION

Medical physics often focuses on techniques to prevent, diagnose, and treat human diseases, including cancers. Medical physics for diagnostic and therapy purposes often involves the utilisation of radiation in the technique to diagnose and treat patients. In radiation study, especially in the medical field, employment of phantom material is necessary to replace a real human body in the verification and measurement of radiation dose received by the patient. Previous studies often reported the usage of various kinds of phantoms in radiation dosimetry and also radiation protection (Katsarou *et al.* 2023; Luo *et al.* 2023).

Phantom is frequently recognised as a model that closely matches the human body and anatomy (Jusufbegović *et al.* 2023), composed of media with close equivalents to human soft tissue (Breslin *et al.* 2023) in terms of size, shape, location, density, and radiation interaction with matter. Dosimetric phantoms are model phantoms that were established in response to the evolution of computational phantoms to quantify and

bioresources.cnr.ncsu.edu

evaluate organ doses after irradiation, either internally or externally. The requirement to imitate the human body in radiation studies has prompted researchers to investigate numerous materials as phantoms; materials that have been declared adequate based on physico-mechanical, attenuation, and scattering investigations.

Characterisation of the phantom is vital to create a phantom that is nearly identical to a real human body, especially in terms of its attenuation and radiation properties. In order to fabricate a comparable phantom, analysis of its properties is necessary to determine the suitability as phantom material, especially in radiation study. Water has been shown to exhibit a similar affinity to soft tissue, and the IAEA has recognised it as a standard phantom. Water has predictable qualities that are suitable for radiation study and is commonly available, thus it is recommended for dosimetry reasons in radiation dosimetry (Samson *et al.* 2023). It is close to soft tissue in terms of mass density. However, the use of water as a phantom in any dosimetry process is quite challenging due to its irregular shape and size. One constraint is the difficulty in locating various types of radiation dosimeters because many of them are unsuitable for use in water. As a result, solid phantoms were created and developed as a replacement for water.

Rhizophora as phantom material has received massive attention due to its close compatibility with water, and with the potential of replacing water as phantom in radiation dosimetry. *Rhizophora* spp. is a type of mangrove tree that grows abundantly in the muddy tidal plain mostly found in the coastal area in Malaysia. The genus *Rhizophora* contains many species of mangrove (Abuarra *et al.* 2014). Although global mangrove distribution has fluctuated throughout geological history, *Rhizophora* spp. can be easily found in Malaysia, as Malaysia is the third among the top 20 mangrove-holding nations (Hamilton and Casey 2016). *Rhizophora* spp. commonly reaches up to five to eight metres, approximately at 16 to 26 feet, but it sometimes can reach up to 30 to 40 metres in height with growth of around 3.3 feet per year in height (Duke 2006).

Rhizophora spp. was first discovered as potential phantom material from the study by Sudin *et al.* (1988). One of the latest investigations of *Rhizophora* as phantom material in high energy studies reported that there is good agreement of the radiological parameters determined using the scattered photon energies between the *Rhizophora* based phantom, solid water phantom, and theoretical values of water (XCOM), reflecting the validation of the Compton scattering technique setup (Samson *et al.* 2023). It is also crucial for a phantom material to be made environmentally friendly, with natural-based adhesives without any release of toxic gases throughout its usage. Thus, it is necessary to fine-tune its development and fabrication in order to produce a natural based phantom material without any inclusion of petroleum-based products, which may be harmful to the environment.

Previous literature reported various fabricated particleboards made of natural-based material, which were produced and analysed as phantom material in radiation study (Zuber *et al.* 2021b). Particleboard as potential phantom requires superior physical and mechanical properties, and in the form of slabs, the rigidity may improve tremendously, as the wood as a whole has natural variations in shape, density and structural integrity due to knots, grain patterns, and other imperfections.

In this work, *Rhizophora*-based particleboard bonded with soy flour and lignin was investigated in terms of its elemental composition, effective atomic number, micrographic structure, computed tomography (CT), and attenuation properties, to determine its suitability as phantom material.

EXPERIMENTAL

Preparation of Particleboard

Rhizophora-based particleboards bonded with different percentages of soy flour and lignin as an adhesive mixture were prepared at different various particle sizes (211 to 500, 104 to 210, 0 to103) µm. Soybean flour (type I) and lignin (alkali, low sulfonate content) (both in powder form) were purchased from Sigma Aldrich, Germany, and used as received. *Rhizophora* wood was first collected from a mangrove factory in Perak, before it underwent several processes – cleaning, debarking, drying, planing, grinding, and sieving to prepare for the fabrication procedure. During the planing process, the trunks were dried and cut further into smaller size using a surface planer machine. The reduced wood chips were then ground into smaller particles using a wood grinder. The particulates were allowed to dry for a few days before being sieved, and they were dried again before hot-pressing. For the fabrication process, hot press was used to produce the particleboard at a target density of 1.0 g·cm^{-3}, at a dimension of approximately $(23.0 \times 23.0 \times 0.5)$ cm^3. Equation 1 (Tousi *et al.* 2014) was used to compute the quantity of each component used in the fabrication of the particleboard,

$$M_W = 7\% \times \rho V - [(M_R \times MC\%_R) + (M_S \times MC\%_S) + (M_L \times MC\%_L)]$$

where,

$$\rho = \frac{M}{V};$$
$$M_R = W_R\% \times \rho V \times (1 + MC\%_R);$$
$$M_S = W_S\% \times \rho V \times (1 + MC\%_S);$$
$$M_L = W_L\% \times \rho V \times (1 + M\%_L) \tag{1}$$

where ρ, ρ_t, M, and V are the density, target density, mass and volume of the sample. $M_R, W_R\%$, and $MC\%_R$ are the mass, weight percentage, and moisture content of *Rhizophora*, $M_S, W_S\%$, and $MC\%_S$ are the mass, weight percentage, and moisture content of soy flour, $M_L, W_L\%$ and $MC\%_L$ represent mass, weight percentage and moisture content of lignin, and M_w is the mass of water.

Elemental Composition Analysis for Adhesive-Bonded Particleboard

Elemental composition of the samples was obtained using scanning electron microscopy with energy dispersive X-ray analysis (SEM-EDXA) (FEI Quanta FEG-650, Netherlands) at the Centre for Global Archaeological Research Earth Material Characterisation Laboratory, Universiti Sains Malaysia. Each sample was fixed onto a specimen holder using a double-sided adhesive tape, and the images were captured under the magnification of $1000 \times$, $2000 \times$ and $4000 \times$. The effective atomic number Z_{eff} was calculated by Eq. 2,

$$Z_{eff} = [\sum_{i=1}^{n}(a_i z_i^m)]^{(\frac{1}{m})} \tag{2}$$

where a_i and z_i are electron fraction and atomic number of the ith element in the sample respectively, and m is the experimental coefficient for biological materials and water with value of 3.4. The electron fraction of the ith element was calculated by Eq. 3,

$$a_i = \frac{w_i\left(\frac{z_i}{A_i}\right)}{\sum w_i\left(\frac{z_i}{A_i}\right)} \quad\quad\quad (3)$$

where w_i and A_i are fractional weight and atomic mass of the ith element, respectively.

Analysis of Micrographic Structure of the Sample in ImageJ

The micrographs of the sample obtained from SEM-EDXA were analysed in ImageJ to evaluate the homogeneity of the particleboard. An average of circular area was obtained from ImageJ software and mean measurement was taken to evaluate the uniformity and homogeneity of the mixture.

CT Analyses of Sample in ImageJ

CT images and density distribution profiles of the particleboard were obtained using a medical X-ray CT scanner (Somatom Definition.AS+, Siemens, Germany). The samples, shaped cylindrically with dimensions approximately 7.0 cm in length and 3.0 cm in diameter, were assembled using wood adhesive. They were trimmed to achieve a smooth cylindrical form, aligning with the section of the CIRS 062 M water-equivalent electron density phantom. Following the production of plug-density phantoms from each sample, they were scanned using a reference water-equivalent plug-density phantom. The plug phantom inserts encompass variations for lung (inhale), adipose tissue, breast, bone, muscle, and liver. All samples were scanned using an X-ray peak energy set at 120 kVp and 187 mAs, utilising a tungsten X-ray target. During the scanning process, Adaptive Iterative Dose Reduction 3D (AIDR 3D) was implemented to minimise radiation dose and noise, while optimising image quality. Subsequently, the images were reconstructed with a filter kernel (FC18, without additional beam hardening correction) at a slice thickness of 1.0 mm. The full field of view image was utilised for each imaging modality. Analysis of the acquired images was conducted using the ImageJ.exe software, wherein the density profiles were generated based on CT raw data to create a plot profile across the phantom volume. A horizontal line was drawn across each plug phantom, and the average densities along the line were derived as shown in Fig. 1.
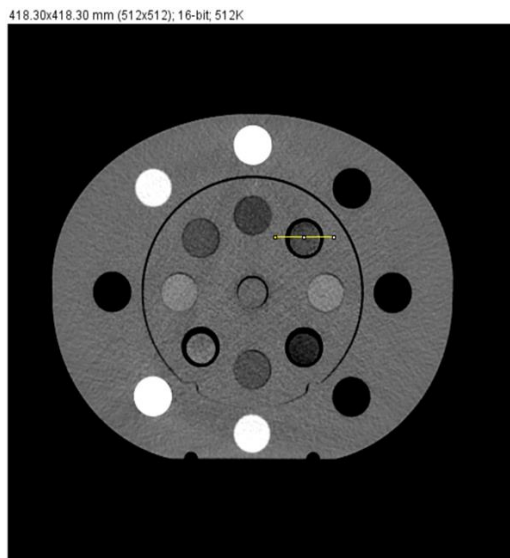

Fig. 1. Line profile for lateral distance measurement and analysis

Attenuation Analyses of Sample Using Monte Carlo GATE

The simulation utilized a custom-built personal computer (PC) with INTEL Core I9 14900K 24 Cores 32 Threads 3.2Ghz LGA1700 Processor with an Ubuntu 22.04.4 LTS operating system (OS) GATE v9.4 including the Geant4 v11.2.1 and Root v6.28/12 platforms. The samples' linear and mass attenuation coefficients were determined using a Ludlum setup with a lead equivalent configuration. The source was positioned inside a shielded container, roughly 30.0 cm away from the Ludlum detector. The detector, which measures about 6.7 cm diameter and 22.9 cm in length, was equipped with a collimator featuring a 0.5 mm diameter and positioned around 30.0 cm above the surface. The sample was placed about 10.0 cm from the Ludlum detector. For this work, samples with a predetermined density of 1.0 g·cm^{-3} were subjected to irradiation with a sealed radiation source of ^{137}Cs, which has an effective peak energy of 0.662 MeV. The setup was generated using GATE software, which utilised macro files to simulate the configuration, adapting the SPECTHead example for this specific work. The setup was modelled using the GATE MC package, simulating 10 million particle histories. After initialising ROOT for output, the simulation data were analysed to count events within a specified energy window. From this data, the linear and mass attenuation coefficients were calculated.

RESULTS AND DISCUSSION

Figure 2 illustrates the preparation of *Rhizophora* raw wood for the fabrication process which include the collection of the wood, cutting, debarking, planing, and grinding of the wood particles. Wood particles were then dried for a few hours up to a few days before the sieving process to prepare samples at three different particle sizes.

Fig. 2. (a) Wood truck collected from mangrove factory; (b) Debarking process of the wood trunk; (c) Planing process to produce wood particles; (d) Wood particle underwent grinding process; (e) Sieving process to prepare the wood particles at different particle sizes

Elemental Analysis for Adhesive-Bonded Particleboard

The elemental composition in atomic, weight percentiles and effective atomic number of *Rhizophora* samples is described in Tables 1 and 2. Figure 3 demonstrates the spectrum processing for each sample.

Based on the result, the elemental composition of the samples in weight percentiles demonstrated high values in carbon and oxygen, representing the natural element of the wood particles, with the formulation of soy flour and lignin as natural-based adhesives. Previous literature reported that the elevated levels of carbon and oxygen in the composites stem from their increased flow rates during high-temperature processing, which is closely tied to the chemical makeup of the samples and holds noteworthy importance in the particleboard phantom (Samson *et al.* 2020). Such attributes contribute to enhanced performance as a dosimetric phantom, yielding superior outcomes in practical applications (Samson *et al.* 2020).

Table 1. Atomic Percentage of the Elemental Composition for Each Sample

Sample	Atomic Fraction of Element (%)											
	C	O	F	Na	Mg	Al	Cl	K	Ca	Ti	Mn	Sr
A_0	57.26	32.20	9.01	0.14	0.14	0.88	-	-	0.21	-	-	0.17
A_6	60.85	37.06	-	0.26	-	0.68	0.28	-	0.38	0.18	-	0.31
A_{12}	59.53	39.00	-	0.22	-	0.56	0.24	0.25	0.14	-	-	0.06
B_0	59.99	38.83	-	-	-	0.39	0.35	-	0.29	-	-	0.14
B_6	59.09	40.38	-	0.10	-	-	0.16	0.08	0.12	-	-	0.06
B_{12}	60.14	37.02	1.86	0.10	0..05	0.24	0.16	0.22	0.15	-	0.06	-
C_0	60.95	36.82	-	0.17	-	1.29	0.29	-	0.28	-	-	0.20
C_6	60.26	38.68	-	0.18	0.06	0.37	0.16	0.08	0.13	-	-	0.09
C_{12}	59.82	39.10	-	0.11	-	0.44	0.15	0.15	0.15	-	-	0.08

A = 211 to 500 µm, B = 104 to 210 µm, C = 0 to 103 µm particle size ranges;
0 = 0% soy flour and lignin, 6 = 4.5% soy flour and 1.5% lignin, 12 = 9% soy flour and 3% lignin

Table 2. Weight Percentage and Effective Atomic Number Z_{eff} of the Elemental Composition for Each Sample

Sample	Weight Fraction of Element (%)												Z_{eff}
	C	O	F	Na	Mg	Al	Cl	K	Ca	Ti	Mn	Sr	
A_0	48.17	36.08	11.98	0.22	0.24	1.66	-	-	0.60	-	-	1.04	10.80
A_6	51.87	42.08	-	0.42	-	1.31	0.71	-	1.08	0.63	-	1.91	12.46
A_{12}	51.52	44.96	-	0.36	-	1.09	0.61	0.71	0.40	-	-	0.35	9.20
B_0	51.88	44.72	-	-	-	0.76	0.90	-	0.83	-	-	0.91	10.09
B_6	51.53	46.91	-	0.17	-	-	0.41	0.23	0.36	-	-	0.39	9.05
B_{12}	52.21	42.8	2.56	0.16	0.09	0.47	0.41	0.62	0.44	-	0.24	-	8.15
C_0	52.33	42.11	-	0.28	-	2.49	0.73	-	0.80	-	-	1.25	11.25
C_6	52.46	44.86	-	0.29	0.1	0.73	0.41	0.21	0.37	-	-	0.56	9.56
C_{12}	51.97	45.25	-	0.18	-	0.86	0.38	0.43	0.42	-	-	0.51	9.51

A = 211 to 500 µm, B = 104 to 210 µm, C = 0 to 103 µm particle size ranges;
0 = 0% soy flour and lignin, 6 = 4.5% soy flour and 1.5% lignin, 12 = 9% soy flour and 3% lignin

There were several metal elements detected in the composition, including strontium, manganese and titanium in small fractions, which may be due to the exposure of the samples towards gold for conductivity during the scanning electron microscopy and energy-dispersive x-ray analyses. However, the minuscule percentile of the metal element

is deemed negligible in this work. In this work, the effective atomic number was calculated and results demonstrated that B_{12} presented with effective atomic number of 8.15, which is the closest to water as compared to other sample. This may be due to the presence of impurities such as the unnecessary metal elements.
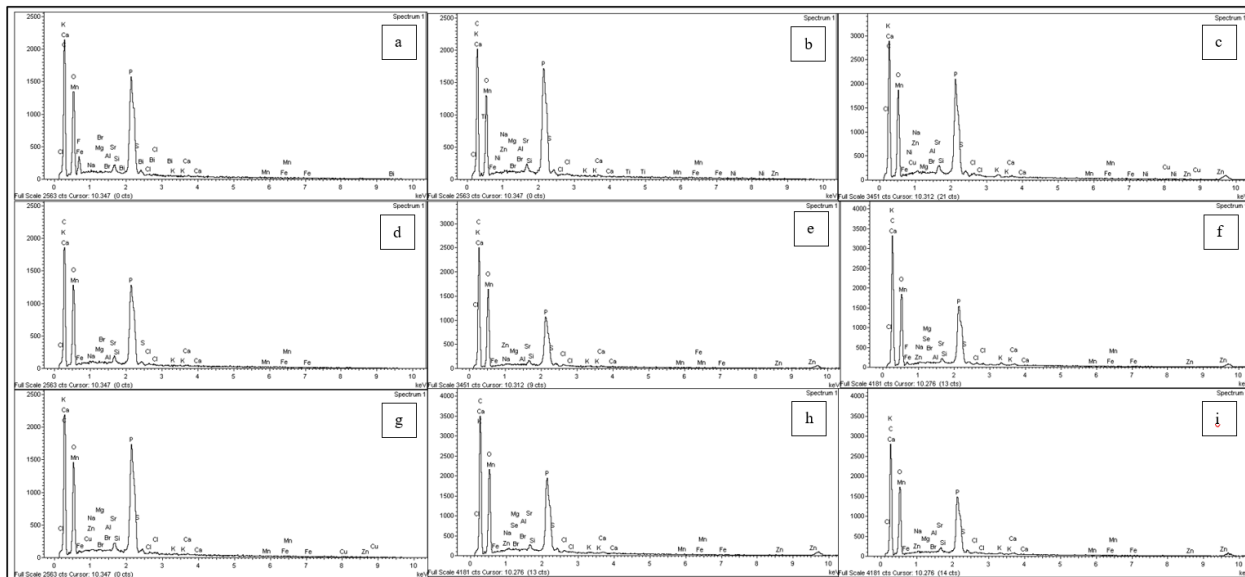

Fig. 3. Spectrum processing for (a) A_0; (b) A_6; (c) A_{12}; (d) B_0; (e) B_6; (f) B_{12}; (g) C_0; (h) C_6; (i) C_{12} in EDX analysis
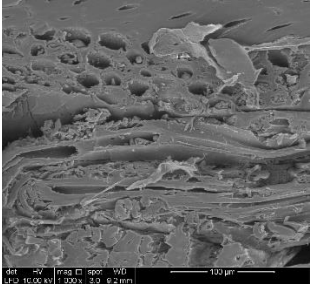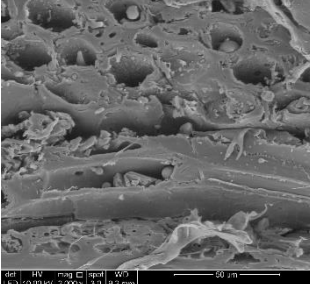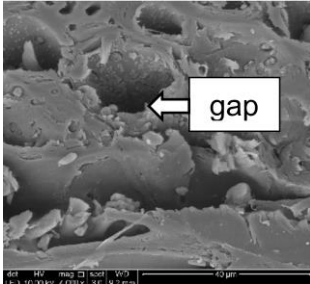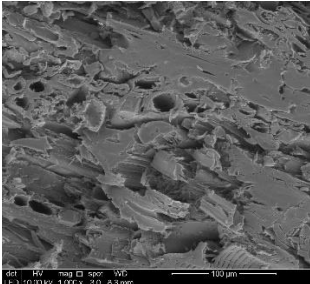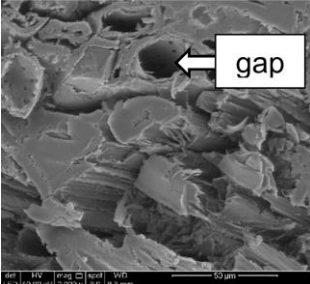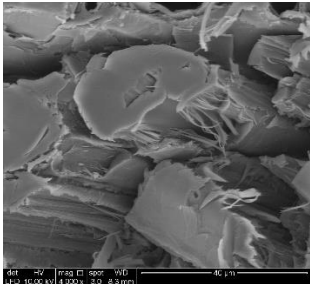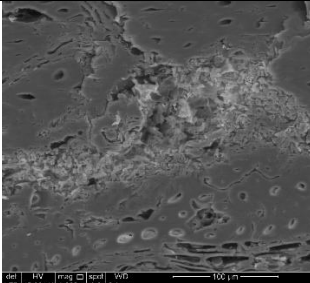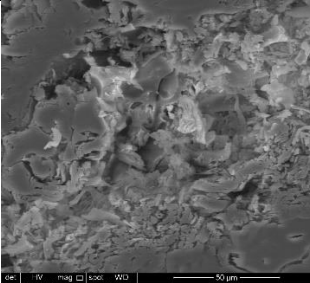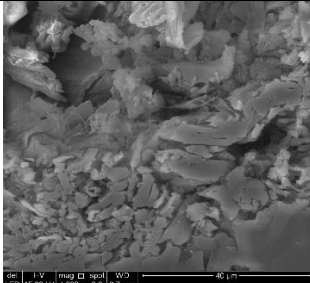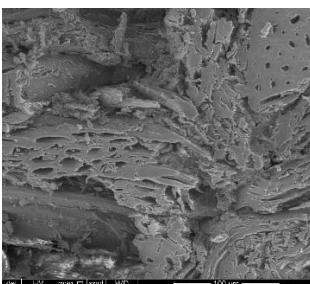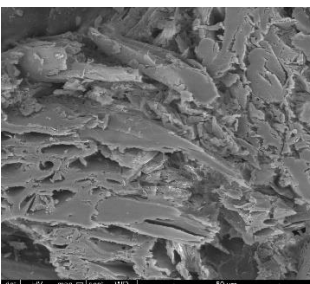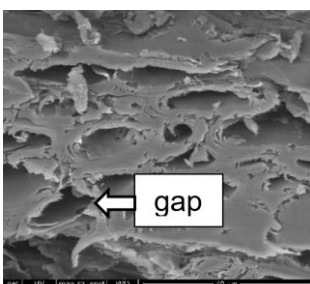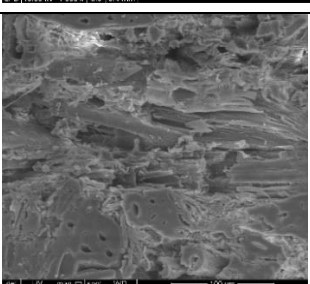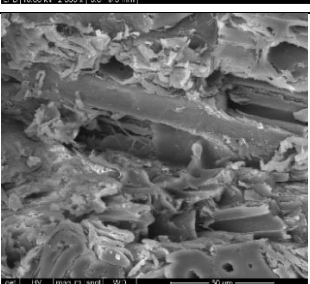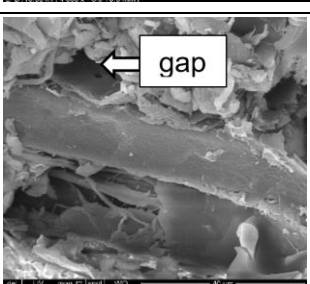
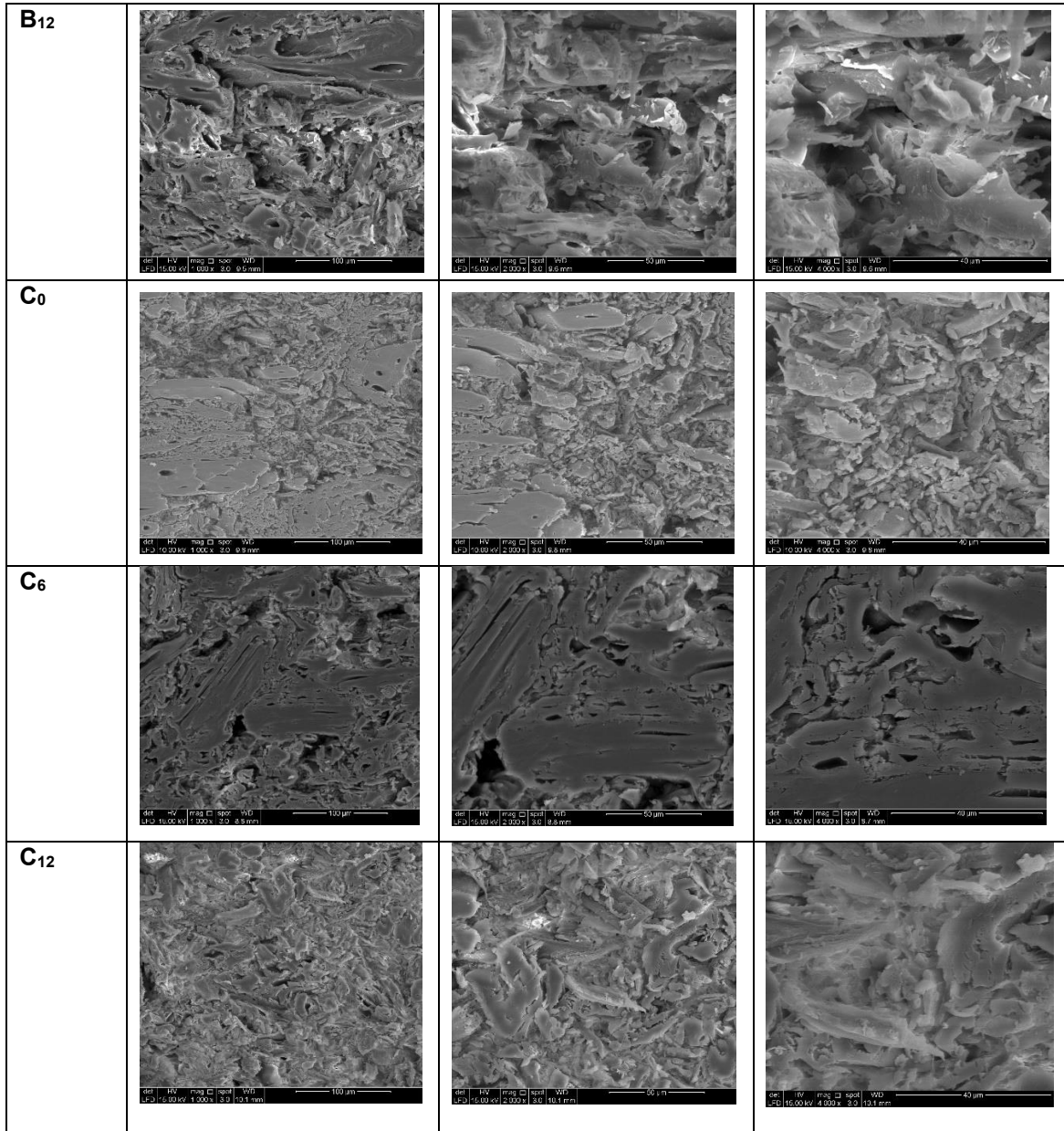## Analysis of Micrographic Structure of the Sample in Imagej

Table 3 illustrates the micrograph of the *Rhizophora* samples at different percentages of soy-lignin adhesives at (a) 1000 × (b) 2000 × and (c) 4000 ×. Based on the figure, sample A_0 presented with discernible void spaces in between the particulates, indicating lack of homogeneity in between the *Rhizophora* wood particles without the presence of adhesive for bonding. The same was observed for B_0 and C_0, whereas, for samples B_6 and $B_{12,}$ it is apparent that the fabricated samples did not reach a satisfactory homogeneity of compounds based on the micrograph, which may indicate the inadequate hot-pressing procedure during the fabrication process. Large void and air gaps presented in samples B_6 and B_{12} suggested weak merging and bonding between the particulate, which requires further processing.

The ImageJ analysis for magnification of 1000 ×, 2000 × and 4000 × is shown in Table 4. Based on the grayscale histogram analysis, C_6 presented the smallest mean, indicating its superior homogeneity compared to other samples. ImageJ software was used to analyse SEM images to study the presence of void spaces in the fabricated sample (Thilagashanthi *et al.* 2021). C_6 demonstrated a compound with little to no void or air gaps, stipulating its potential as phantom material. Multiple void spaces presented in the micrograph elucidate the inhomogeneity and non-uniformity within the compound post-hot-pressing, which may affect its physical and mechanical strength. Previous literature reported that the presence of voids resulting from lumen and hole formation in composites can cause uneven distribution and decreased density (Samson *et al.* 2020). The incorporation of adhesives in the formulation stipulated the improved inhomogeneity, as manifested in C_6, with potential of enhanced physical and mechanical properties (Samson *et al.* 2020). It is crucial for phantom material made from particleboard to be superior in

mechanical stability. This will allow for a higher usage rate, thus contributing to cost-effectiveness.

Table 3. Micrograph of the *Rhizophora* Samples at Different Percentages of Soy-Lignin Adhesives at (a) 1000 × (b) 2000 × and (c) 4000 ×

Sample	Magnification		
	1000 ×	**2000 ×**	**4000 ×**
A_0			
A_6			
A_{12}			
B_0			
B_6			

A = 211 to 500 µm, B = 104 to 210 µm, C = 0 to 103 µm particle size ranges;
0 = 0% soy flour and lignin, 6 = 4.5% soy flour and 1.5% lignin, 12 = 9% soy flour and 3% lignin

Table 4. The ImageJ analysis at 1000 ×, 2000 × and 4000 × Magnification

Sample	Magnification at 1000 ×				Magnification at 2000 ×				Magnification at 4000 ×			
	Area	Mean	Min	Max	Area	Mean	Min	Max	Area	Mean	Min	Max
A_0	144.606	105.750	24	208	139.545	100.133	29	209	166.116	94.542	27	214
A_6	148.577	96.133	17	212	169.337	94.201	22	200	174.351	98.071	20	198
A_{12}	156.529	94.588	23	197	162.564	103.658	27	224	153.701	99.926	21	191
B_0	131.420	108.589	26	237	155.192	114.568	28	255	155.699	115.082	32	230
B_6	129.513	100.914	32	191	183.078	99.191	18	255	150.376	115.654	26	244
B_{12}	140.125	102.383	0	255	158.542	92.220	4	255	156.375	107.336	1	248
C_0	152.558	121.695	35	234	152.573	120.602	37	236	159.916	123.244	38	229
C_6	143.331	67.544	0	172	160.632	69.302	1	144	145.888	73.472	0	150
C_{12}	143.401	102.850	8	217	146.534	109.150	20	241	155.813	106.965	34	183

A = 211 to 500 µm, B = 104 to 210 µm, C = 0 to 103 µm particle size ranges;
0 = 0% soy flour and lignin, 6 = 4.5% soy flour and 1.5% lignin, 12 = 9% soy flour and 3% lignin

CT Analyses of Sample in Image J

The CT numbers given by the Hounsfield unit (HU) were a result of the density of the material used and the scale range from -1000 (indicating darker shades) to +1000 (indicating lighter shades). Lower density causes darker shades of grey, whereas higher density value produces lighter shades. The HU value of air is -1000, and denser material, such as bone, has a value of +1000. Water has an HU value of 0, and the HU of soft tissue ranges from -200 to +200 (Sichel *et al.* 2000). Based on the average CT number, the closest CT number to water was recorded by C_{12}, (Zuber *et al.* 2021a) indicating that C_{12} has comparable attenuation properties to water. These results align with previous studies (Marashdeh *et al.* 2012; Mohd Yusof *et al.* 2017).

CT numbers between -200 and +200 HU were similar to water and soft tissues (Zuber *et al.* 2021a). The mean CT number may be affected by the inconsistent application of adhesives in the sample. Larger discrepancies occurred when the value was compared with other average CT number, indicating lack of homogeneity due to larger particles. However, all the samples were within the required CT number for soft tissue. Figure 4 shows the fabricated plug phantom, whereas Fig. 5 illustrates the CT images of the plug phantom at various percentages of soy flour and lignin at different particle sizes. The electron density profiles of the samples are shown in Figs. 6 through 8.

Fig. 4. Fabricated plug phantom at different percentages of adhesives and different particle sizes

Close proximity of densities across the plug phantoms can be seen at 0 to 103 µm particle sizes, as compared to plug phantom at bigger particle sizes, in sample bonded with 12% adhesives. The same goes with plug phantom bonded with 6% adhesives. Based on the figures, the density distribution profile of adhesive bonded samples presented with close proximities to those of water at the smallest particle sizes of 0 to 103 µm, with C_6 to be the closest of them all. The density profile of binderless sample at 104 to 210 µm particle sizes also was revealed to be closest to those of water. In this study, uniformity across the profile can be observed for majority of the samples, indicating little variation in the uniformity of the fabricated samples. This is largely attributed to the methodology employed during the formulation mixing, cold-pressing, and hot-pressing processes. Disparity in terms of density for both adhesives may result in a heterogeneous grayscale appearance if not thoroughly mixed within the plug phantom.
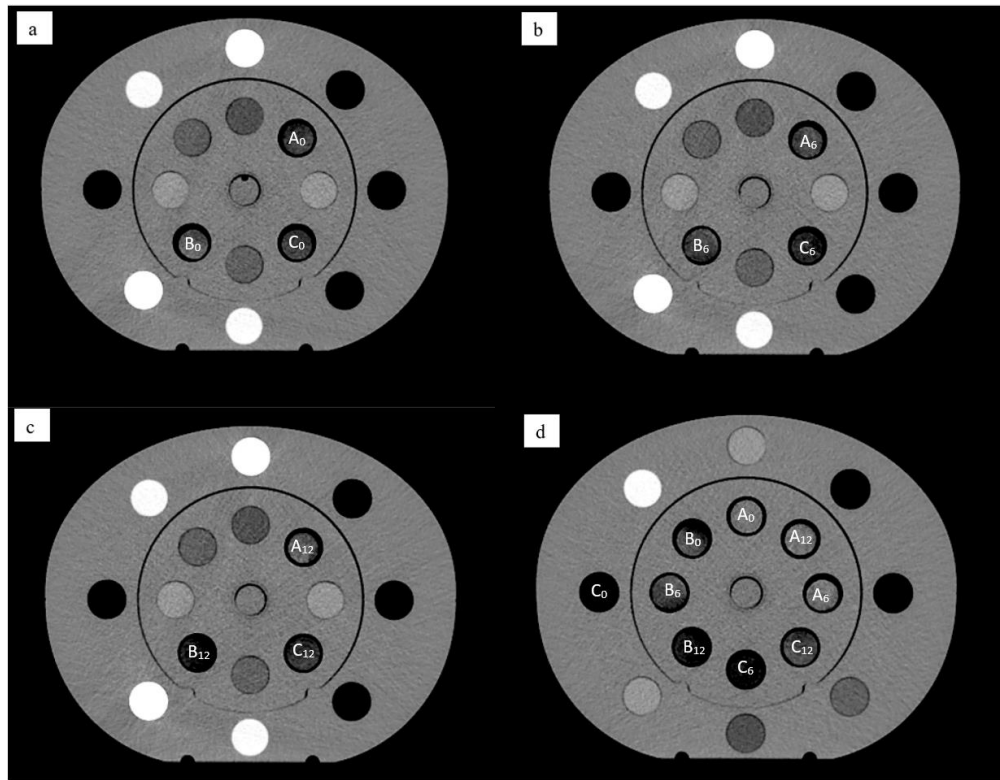
Fig. 5. CT images of fabricated plug phantoms at various percentages of soy flour and lignin and at different particle sizes
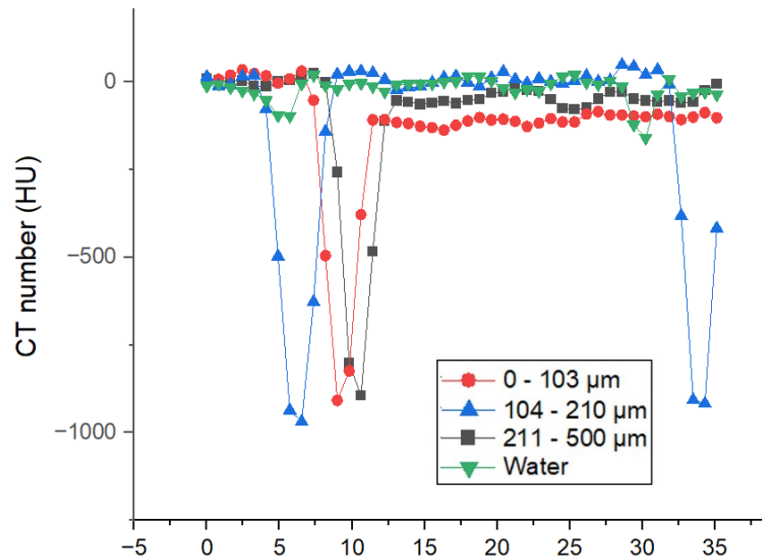

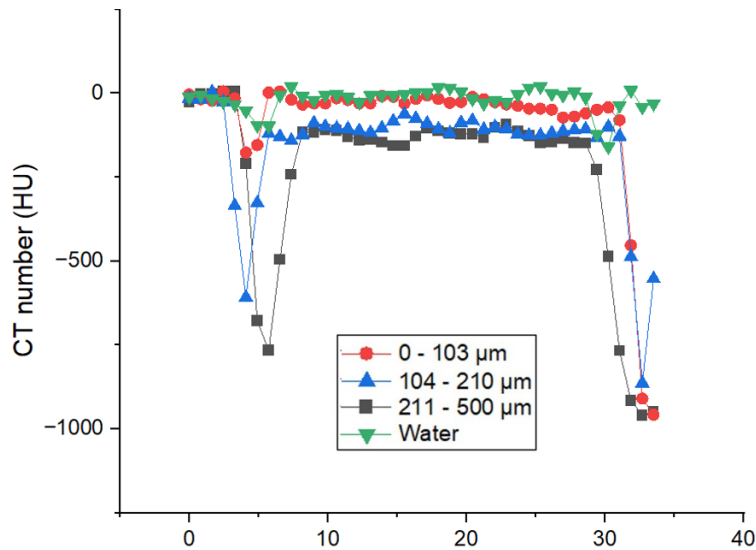**Fig. 6.** Density profiles for binderless samples

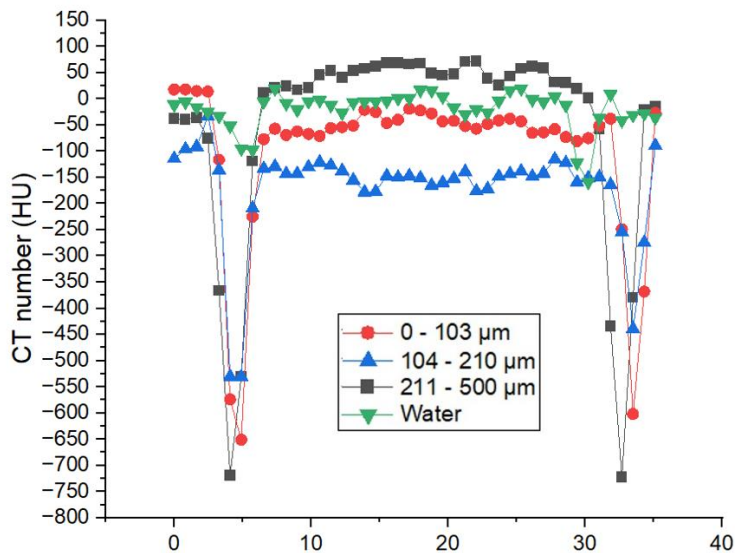**Fig. 7.** Density profile for samples with 6% adhesives

Fig. 8. Density profile for samples with 12% adhesives

A previous study reported a resulting dose difference of 1% for an electron density difference of 8% for typical radiotherapy beams, whereas another study reported 21% difference in electron density resulted in 2.6% dose difference (Thomas 1999; Hatton *et al.* 2009). Overall, the results revealed that the density distribution profile of the plug phantom closely matches that of water, suggesting its suitability as a phantom material for medical physics applications.

Attenuation Analyses of Sample using Monte Carlo GATE

Figure 9 shows the geometric arrangement of the lead equivalent configuration as modelled in GATE. Table 5 depicts the linear and mass attenuation coefficients of the samples in comparison to those of water calculated with the XCOM. The measured attenuation coefficients were aligned closely with those of water, as determined by XCOM, a widely recognised database for photon cross sections, with C_{12} and A_{12} presented with the closest values to water.
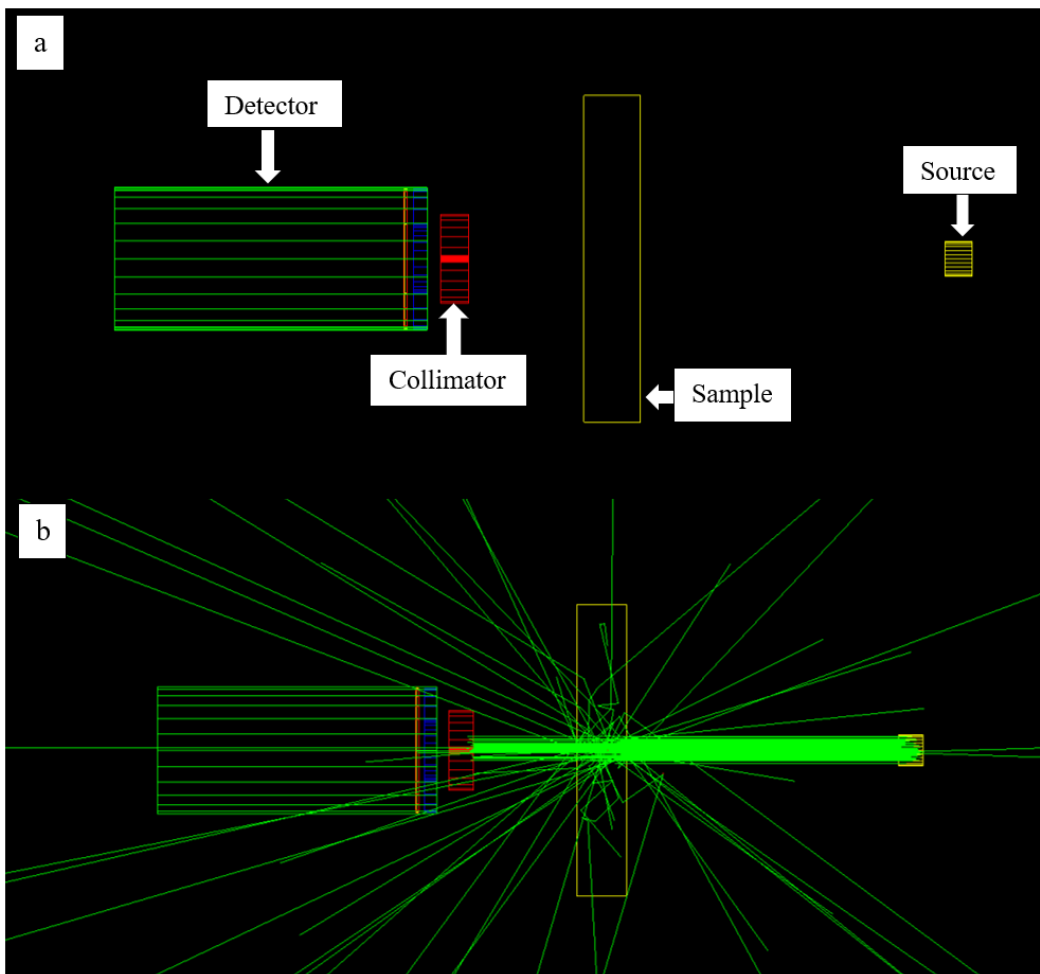
Fig. 9. (a) Geometric arrangement of the lead equivalent configuration as modeled in GATE; (b) Visualisation of energy transmission for attenuation simulated in GATE

Table 5. Simulated Linear and Mass Attenuation Coefficients of the Samples in Comparison to Those of Water Calculated with the XCOM

Sample	Average Density (g·cm⁻³)	^{137}Cs (0.662 MeV)	
		μ (cm⁻¹)	μ/ρ (cm²g⁻¹)
A_0	1.000	0.0772	0.0772
A_6	1.000	0.0763	0.0763
A_{12}	1.000	0.0781	0.0781
B_0	1.000	0.0766	0.0766
B_6	1.000	0.0771	0.0771
B_{12}	1.000	0.0762	0.0762
C_0	1.000	0.0772	0.0772
C_6	1.000	0.0764	0.0764
C_{12}	1.000	0.0780	0.0780
Water (XCOM)	1.000	0.0860	0.0860

A = 211 to 500 μm, B = 104 to 210 μm, C = 0 to 103 μm particle size ranges;
0 = 0% soy flour and lignin, 6 = 4.5% soy flour and 1.5% lignin, 12 = 9% soy flour and 3% lignin
μ (cm⁻¹) = linear attenuation coefficient, μ/ρ (cm²g⁻¹) = mass attenuation coefficient

This alignment is particularly noteworthy because water is used as a reference standard in radiological studies due to its compositional similarities to human soft tissue (Büyükyıldız *et al.* 2024). This close agreement is significant because water's attenuation properties are often used as a benchmark in radiological contexts, given its similarity to human soft tissue in terms of composition and density (Zuber *et al.* 2021b). Thus, the material in question closely mimics the radiological properties of human soft tissue.

Human soft tissues, such as muscle, fat, and organs, consist largely mainly of water (Meher *et al.* 2024), contributing to their similar radiological behavior. Thus, materials that exhibit attenuation coefficients close to those of water are likely to replicate the interaction between human tissues and ionising radiation accurately. Such materials are excellent candidates for use as tissue-equivalent materials in medical physics applications. By closely mimicking the radiological properties of human tissues, these materials can be used in the calibration and testing of medical imaging devices, as well as in research and training settings (McGarry *et al.* 2020). This enables more accurate dosimetry, improved imaging techniques, and better training tools which are crucial for advancing medical technology and ensuring patient safety during radiological procedures. Hence, the close agreement between the measured coefficients and those of water supports the potential of the evaluated material to serve as a realistic surrogate for human tissue in various medical physics applications.

CONCLUSIONS

1. The findings highlight the promising potential of *Rhizophora*-based particleboard, bonded with soy flour and lignin, for medical physics applications with good physical and mechanical properties.

2. The C_6 sample exhibited good uniformity and homogeneity, indicating its potential as a phantom material.

3. Notably, the B_{12} sample demonstrated an effective atomic number of 8.15, closely resembled that of water, suggesting its suitability for medical physics applications.

4. The C_6 also exhibited a density distribution profile that closely resembled that of water.

5. The attenuation coefficients of the samples closely matched those of water, as determined by XCOM.

ACKNOWLEDGMENTS

REFERENCES CITED

Abuarra, A., Hashim, R., Bauk, S., Kandaiya, S., and Tousi, E. T. (2014). "Fabrication and characterization of gum Arabic bonded *Rhizophora* spp. Particleboards," *Mater. Des*. 60, 108-115.

Breslin, T., Paino, J., Wegner, M., Engels, E., Fiedler, S., Forrester, H., Rennau, H., Bustillo, J., Cameron, M., Häusermann, D., Hall, C., Krause, D., Hildebrandt, G., Lerch, M., and Schültke, E. (2023). "A novel anthropomorphic phantom composed of tissue-equivalent materials for use in experimental radiotherapy: Design, dosimetry and biological pilot study," *Biomimetics* 8(2), 230 DOI: 10.3390/biomimetics8020230

Büyükyıldız, M., Kaur, P., Thakur, S., and Atlı, R. (2024). "Study of phantom materials close to 1 keV photon energy for radiation applications," *Radiat. Phys. Chem.* 215, article 111375. DOI: 10.1016/j.radphyschem.2023.111375

Duke, N. C. (2006). "Indo-West Pacific stilt mangroves: *Rhizophora apiculata*, *R. mucronata*, *R. stylosa*, *R. X annamalai*, *R. X lamarckii*," Permanent Agriculture Resources (PAR).

Hamilton, S. E., and Casey, D. (2016). "Creation of a high spatio-temporal resolution global database of continuous mangrove forest cover for the 21st century (CGMFC-21)," *Glob. Ecol. Biogeogr*. 25, 729-738.

Hatton, J., McCurdy, B., and Greer, P. B. (2009). "Cone beam computerized tomography: the effect of calibration of the Hounsfield unit number to electron density on dose calculation accuracy for adaptive radiation therapy," *Phys. Med. Biol.* 54, N329-46. DOI: 10.1088/0031-9155/54/15/N01

Jusufbegović, M., Pandžić, A., Busuladžić, M., Čiva, L.M., Gazibegović-Busuladžić, A., Šehić, A., Vegar-Zubović, S., Jašić, R., and Beganović, A. (2023). "Utilisation of 3D printing in the manufacturing of an anthropomorphic paediatric head phantom for the optimisation of scanning parameters in CT," *Diagnostics* 13(2), article 328. DOI: 10.3390/diagnostics13020328

Katsarou, M., Zwiebel, B., Chowdhury, R.P., Shames, M., Berger, T., Przybyla, B., and Bismuth, J. (2023). "Experimental analysis of radiation protection offered by a novel exoskeleton-based radiation protection system *versus* conventional lead aprons," *J. Vasc. Interv. Radiol.* 34(8), 1345-1352 DOI: 10.1016/j.jvir.2023.03.033

Luo, X., Qiu, R., Wu, Z., Yan, S., Zhang, H., and Li, J. (2023). "A body-size-dependent series of Chinese adult standing phantoms for radiation dosimetry," *J. Radiol. Prot.* 43, article 11501. DOI: 10.1088/1361-6498/acad0d

Marashdeh, M. W., Bauk, S., Tajuddin, A. A., and Hashim, R. (2012). "Measurement of mass attenuation coefficients of *Rhizophora* spp. binderless particleboards in the 16.59–25.26keV photon energy range and their density profile using x-ray computed tomography," *Appl. Radiat. Isot.* 70, 656-662. DOI: 10.1016/j.apradiso.2012.01.008

McGarry, C. K., Grattan, L. J., Ivory, A. M., Leek, F., Liney, G. P., Liu, Y., Miloro, P., Rai, R., Robinson, A., Shih, A. J., Zeqiri, B., and Clark, C. H. (2020). "Tissue mimicking materials for imaging and therapy phantoms: A review," *Phys. Med. Biol*. 65(23), 23TR01 DOI: 10.1088/1361-6560/abbd17

Meher, A. K., Kumar, E. K., Gangwar, A., Panda, S. K., and Pradhan, R. C. (2024). "Review on mechanobiological analysis and computational study of human tissue (soft and hard) using machine learning techniques: A mechanical perspective," *Arch. Comput. Methods Eng.* 31, 957-972. DOI: 10.1007/s11831-023-10003-4

Samson, Damilola Oluwafemi, Aziz, M. Z. A., Shukri, A., Jafri, M. Z. M., Hashim, R., Zuber, S. H., Hashikin, N. A. A., Rabba, J. A., Samson, P. A., and Yusof, M. F. M. (2023). "Radiological and dosimetric evaluation of biomaterial composite phantoms with high energy photons and electrons," *Health Phys.* 10-1097.

Samson, D. O., Jafri, M. Z. M., Shukri, A., Hashim, R., Sulaiman, O., Aziz, M. Z. A., and Yusof, M. F. M. (2020). "Measurement of radiation attenuation parameters of modified defatted soy flour–soy protein isolate-based mangrove wood particleboards to be used for CT phantom production," *Radiat. Environ. Biophys.* 59, 483-501. DOI: 10.1007/s00411-020-00844-z

Samson, Damilola O, Shukri, A., Hashikin, N. A. A., Zuber, S. H., Aziz, M. Z., Hashim, R., Yusof, M. F., Rabaiee, N. A., and Gemanam, S. J. (2023). "Dosimetric characterization of DSF/NaOH/IA-PAE/R. spp. phantom material for radiation therapy," *Polymers (Basel)*. DOI: 10.3390/polym15010244

Sichel, J. Y., Dangoor, E., Eliashar, R., Aksoy, F. G., Dano, I., and Gomori, M. (2000). "Artifactual thickening of the sinus walls on computed tomography: a phantom model and clinical study," *Ann. Otol. Rhinol. Laryngol.* 109, 859-862. DOI: 10.1177/000348940010900914

Sudin, C., Tajuddin, A. A., and Bradley, D. A. (1988). "Evaluation of tissue-equivalent media for dosimetric studies," in: *Proceeding of Local Seminar Activities on Radiation Physics, Biophysics and Medical Physics*, Kuala Lumpur, Malaysia. pp. 71-80.

Thilagashanthi, T., Gunasekaran, K., and Satyanarayanan, K. S. (2021). "Microstructural pore analysis using SEM and ImageJ on the absorption of treated coconut shell aggregate," *J. Clean. Prod.* 324, 129217. DOI: 10.1016/j.jclepro.2021.129217

Thomas, S. J. (1999). "Relative electron density calibration of CT scanners for radiotherapy treatment planning," *Br. J. Radiol.* 72, 781-786. DOI: 10.1259/bjr.72.860.10624344

Tousi, E. T., Hashim, R., Bauk, S., Jaafar, M. S., Abuarra, A. M. H., and Ababneh, B. (2014). "Some properties of particleboards produced from *Rhizophora* spp. as a tissue-equivalent phantom material bonded with *Eremurus* spp.," *Measurement* 54, 14-21. DOI: 10.1016/j.measurement.2014.04.004

Yusof, M. F. M., Hashim, R., Tajuddin, A. A., Bauk, S., and Sulaiman, O. (2017). "Characterization of tannin-added *Rhizophora* spp. particleboards as phantom materials for photon beams," *Ind. Crops Prod.* 95, 467-474. DOI: 10.1016/j.indcrop.2016.10.057

Zuber, S. H., Hashikin, N. A. A., Mohd Yusof, M. F., Aziz, M. Z. A., and Hashim, R. (2021a). "Characterization of soy-lignin bonded *Rhizophora* spp. particleboard as substitute phantom material for radiation dosimetric studies - Investigation of CT number, mass attenuation coefficient and effective atomic number," *Appl. Radiat. Isot.* 170, 109601. DOI: 10.1016/j.apradiso.2021.109601

Zuber, S. H., Yusof, M. F. M., Hashikin, N. A. A., Samson, D. O., Aziz, M. Z. A., and Hashim, R. (2021b). "*Rhizophora* spp. as potential phantom material in medical physics applications – A review," *Radiat. Phys. Chem*. 189, article 109731. DOI: 10.1016/j.radphyschem.2021.109731